Driving Force of Photoinduced Charge Separation in Metal-Cluster Encapsulated Triphenylamine-[80]fullerenes

Juan Pablo Martínez,[1] Miquel Solà[1*] and Alexander Voityuk[1,2*]

[1]*Institut de Química Computacional i Catàlisi and Departament de Química, Campus de Montilivi, 17003 Girona, Catalonia, Spain.*

[2]*ICREA, Pg. Lluís Companys 23, 08010 Barcelona, Catalonia, Spain*

E-mail: miquel.sola@udg.edu, alexander.voityuk@icrea.cat

Abstract

Understanding of photoinduced charge separation in fullerene-based dye-sensitized solar cells is crucial for the development of photovoltaic devices. In this work, we explore how the driving force of the charge separation process in conjugates of $M@C_{80}$ (M = Sc_3N, Sc_3CH, Sc_3NC, Sc_4O_2, and Sc_4O_3) with triphenylamine (TPA) depends on the nature of the metal cluster. Both singlet and triplet excited state electron transfer reactions are considered. Our results based on TD-DFT calculations demonstrate that the driving force of charge separation in TPA-$M@C_{80}$ can be well tuned by varying the structure of the metal cluster encapsulated inside the fullerene cage.

1 Introduction

The present energetic, environmental, and economic crisis has stimulated the interest in developing inexpensive renewable energy sources. Among these sources, solar energy is expected to play a critical role in helping us to meet the current and future global energy demands. In this framework, the dye-sensitized solar cell (DSSC), a photovoltaic cell with potential commercial applications that could compete with existing photovoltaic devices, has strongly transformed the photovoltaic landscape. DSSCs are usually 10-µm-thick, optically transparent film of titanium dioxide particles of a few nm in size, coated with a monolayer of a charge transfer dye to sensitize the film for light harvesting. DSSCs exhibit large current densities (greater than 12 mA/cm^2) and exceptional stability as well.[1] Fullerenes and derivatives have emerged as promising materials for the design of efficient DSSCs.[2–13] The reason can be attributed to the fact that fullerene-based materials are a low-cost alternative for silicon-based solar cells and they are associated to profitable manufacturing and negligible toxicity.[14–19]

Two different types of DSSCs are usually distinguished: bulk heterojunctions[20] (BHJs) where the donor and acceptor (D/A) moieties are not covalently connected, and molecular heterojunctions[21] (mHJs) with covalently linked donor-acceptor (D-A) fragments. Several experimental and theoretical studies have been focused on the blends of poly(3-hexylthiophene) (P3HT) and [6,6]-phenyl-C_{61}-butyric acid methyl ester (PCBM);[17,22–30] however, detailed information of charge transfer (CT) processes can be also extracted from mHJs since a better structural control and charge mobility tuning can be achieved within this approach. Endohedral metallofullerenes (EMFs) have been used in mHJs as electron acceptor groups because they possess larger absorption coefficients than C_{60} in the visible region. This property together with the low reorganization energy[13,31] make them suitable candidates for mHJs. Most studies involving EMFs employ $Sc_3N@I_h$-C_{80} because it is the most abundant EMF.[32] In fact, $Sc_3N@C_{80}$ has been studied in D-A dyads linked to ferrocene, phthalocyanine, tetrathialfulvalene, and triphenylamine (TPA).[33–36] In the particular case of TPA as the donor moiety, Echegoyen et al. performed electrochemical and photophysical studies in mHJs constituted by TPA (the electron donor) and fullerene cages (C_{60} and $Sc_3N@C_{80}$, the electron acceptors) from which they revealed valuable information for the understanding of the CT processes occurring in fullerene DSSCs.[36] Indeed, Echegoyen et al. found that TPA-$Sc_3N@C_{80}$ generates longer-lived CT states than does TPA-C_{60}; consequently, the charge recombination (CR) reaction in the former is slower and the driving force was attributed to be the key factor determining the rate of the reaction.[36] TPA and derivatives have been used as photoactive molecules during several decades and their applicability in the construction of DSSCs is also of technological interest.[37–42] Moreover, TPA and derivatives can retain cationic charge and hamper aggregation between molecules, which induce self-quenching and reduce the electron injection efficiency thus promoting a longer separation of charge.[39,41] On the other hand, EMFs are excellent electron acceptors[33,36,43–46] that react with a variety of chemical agents.[47–54] Consequently, the covalent junctions between TPA and fullerene cages result in interesting assemblies due to: (i) they show, after photoinduction, ultrafast charge separation (CS) reactions in which the lowest-energy excited state entirely localized at the (endohedral)fullerene cage, D-A*, can be efficiently dissociated to form an excited state with strong CT character (i.e., D-A* → D^{1+}-A^{1-}); (ii) the variation of the distance between the D-A interface has an impact in the rate of CT reactions: the shorter the D-A distance, the faster the CT reaction; (iii) nonpolar solvents bring about lack of CT activity since D-A* → D^{1+}-A^{1-} becomes an uphill process; on the contrary, more polar solvents diminish the rate of CR reaction thus delaying the recovery of the ground state (i.e., the rate decreases for D^{1+}-A^{1-} → D-A).

In this contribution, we aim to characterize excited states and explore the effect of the driving force on photoinduced CS reactions in a series of D-A conjugates constituted by TPA and the EMF M@C_{80} with a scandium-based cluster encapsulated inside the cage (see Figure 1; M = Sc_3N, Sc_3CH, Sc_3NC, Sc_4O_2, and Sc_4O_3). It should be noted that for systems containing transition metals the rate constant for intersystem crossing can be much larger (by factor of 10^6) as compared with related organic molecules.[55,56] In view of that, CS reactions in TPA-M@C_{80} are analyzed by considering both singlet and triplet excited states. For the C_{80} cage encapsulating the metal clusters, we have considered the one having icosahedral symmetry (I_h-C_{80}) throughout this work. We anticipate here that we have found that the nature of the cluster plays an essential role in the charge separation processes.

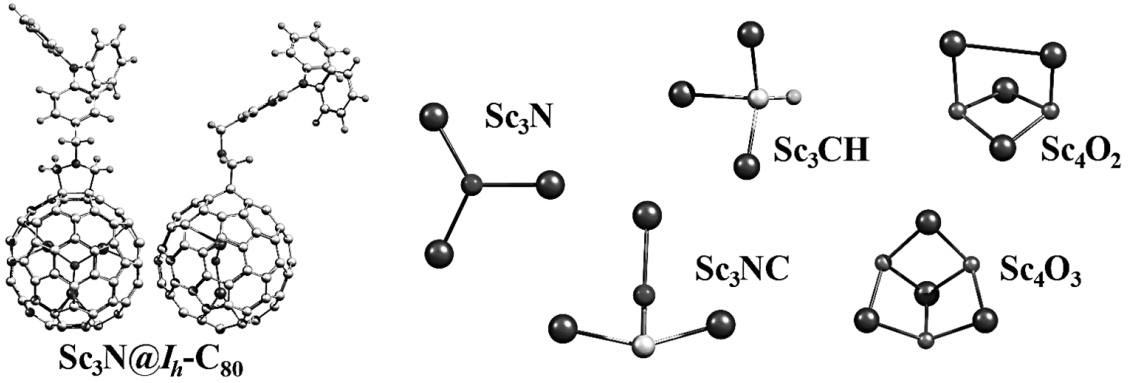

Figure 1 TPA-M@C_{80} structures under study. All these M@C_{80} cages have been experimentally detected.[12,57–61]

2 Methods

The ground-state geometry for each structure TPA-M@C_{80} was optimized using the Gaussian 09 program[62] at the CAM-B3LYP[63]/6-31G*~SDD[64,65] level of theory in implicit solvent (COSMO[66]:benzonitrile). The SDD pseudopotentials were used only for the Sc atom. The geometry of the metallic clusters corresponds to that experimentally observed in the isolated M@C_{80} cage.[12,57–61] The orientation of the metallic cluster with respect to the pyrrolidine ring corresponds to the most stable orientation determined for Diels-Alder adducts.[67] We assumed that this orientation is the same for these 1,3-dipolar adducts (see Table S1), which was confirmed for the complex TPA-Sc_3N@C_{80}. It is worth noting that in TPA-M@C_{80} the rotation of the metal cluster M is partially hindered.[67] Moreover, in the case of the Zn tetraphenyl porphyrin Sc_3N@C_{80} conjugate, Baruah et al. observed that the cluster orientation has a negligible effect on the excitation energies of charge-separated (**CS**) states.[68] Table S2 shows that the geometry of TPA-Sc_3CH@C_{80}, for instance, optimized in the gas phase is almost the same as the solvated one with a calculated root-mean-square deviation (RMSD) of 0.27 Å (in Table S2 the superposition between these geometries is also schematized). Moreover, B3LYP[69,70] and CAM-B3LYP geometries are found to be nearly identical. Our previous study of excited states for several thermally-accessible conformations of TPA-C_{60} revealed that the structural variability of these TPA-fullerene interfaces does not significantly affect the electronic properties of excited states.[71] It has been also postulated that CS reactions in organic photovoltaic interfaces are mostly purely electronic processes.[72] Thus our analysis of TPA-M@C_{80} appears to remain valid even though the effect of the structural fluctuations is not included.[73,74]

The lowest-in-energy one hundred singlet excited states and sixty triplet excited states for each complex were calculated using the CAM-B3LYP/6-31G* scheme in the framework of the time dependent density functional theory (TD-DFT) formalism. The quantitative analysis of exciton delocalization and charge separation in the donor-acceptor complexes was carried out using a tool suggested recently by Plasser et al.[75] A key quantity is the parameter Ω:

$$\Omega(\mathrm{D},\mathrm{A}) = \frac{1}{2}\sum_{\alpha\in\mathrm{D},\,\beta\in\mathrm{A}}\left[\left(\mathrm{SP}^{0\mathrm{i}}\right)_{\alpha\beta}\left(\mathrm{P}^{0\mathrm{i}}\mathrm{S}\right)_{\alpha\beta} + \mathrm{P}^{0\mathrm{i}}_{\alpha\beta}\left(\mathrm{SP}^{0\mathrm{i}}\mathrm{S}\right)_{\alpha\beta}\right], \tag{1}$$

where **S** is the overlap matrix and $\mathbf{P}^{0i}$ the transition density matrix for a $\psi_0 \rightarrow \psi_i$ excitation. The extent of exciton localization *X* on the donor and acceptor is defined by $X_D = \Omega$ (D,D) and $X_A = \Omega$ (A,A). Alternatively, the charge transfer from donor to acceptor, $q(\mathrm{D}\rightarrow\mathrm{A})$, is represented by Ω(D,A), whereas $q(\mathrm{A}\rightarrow\mathrm{D}) = \Omega(\mathrm{A},\mathrm{D})$. The weight of CT states in ψ_i is equal to Ω(D,A) + Ω(A,D) whereas the charge separation Δ*q* between D and A may be determined as the difference $q(\mathrm{D}\rightarrow\mathrm{A})$ - $q(\mathrm{A}\rightarrow\mathrm{D})$ = Ω(D,A) - Ω(A,D). Note that $X_D + X_A + \mathrm{CT} = 1$.

The equilibrium solvation energy $\mathrm{E}_\mathrm{S}^{\mathrm{eq}}$ in medium with the dielectric constant ε was estimated using a COSMO-like polarizable continuum model (C-PCM) in monopole approximation:[76]

$$-\mathrm{E}_\mathrm{S}^{\mathrm{eq}}(\mathrm{Q},\varepsilon) = -\frac{1}{2}\,f(\varepsilon)\mathrm{Q}^{+}\mathrm{D}\mathrm{Q}, \tag{2}$$

where $f(\varepsilon)$ is the dielectric scaling factor, $f(\varepsilon) = \dfrac{\varepsilon - 1}{\varepsilon}$, **Q** the vector of *n* atomic charges in the molecular system, **D** is the *n* x *n* symmetric matrix determined by the shape of the boundary surface between solute and solvent; $\mathbf{D}=\mathbf{B}^{+}\mathbf{A}^{-1}\mathbf{B}$, where the *m* x *m* matrix **A** describes electrostatic interactions between *m* surface charges and the *m* x *n* **B** matrix describes the interaction of the surface charges with *n* atomic charges of the solute. The GEPOL93 scheme was used to construct the molecular boundary surface.[77]

The non-equilibrium solvation energy for excited state ψ_i can be estimated as:[78]

$$\mathrm{E}_\mathrm{S}^{\mathrm{neq}}(\mathrm{Q}^0,\Delta,\varepsilon,\mathrm{n}^2) = f(\varepsilon)\Delta^{+}\mathrm{D}\mathrm{Q}^0 - \frac{1}{2}\,f(\mathrm{n}^2)\Delta^{+}\mathrm{D}\Delta, \tag{3}$$

In Eq. (3), n^2 (the squared refraction index) is the optical dielectric constant of the medium and the vector Δ describes the change of atomic charges in the molecule by excitation.

Changes in electronic energy, ΔE_{ct}, for CT reactions are assumed to be nearly equal to changes in Gibbs energy, ΔG_{ct}, (the entropic term for all compounds is expected to be very similar). In a previous study, we noted that the relaxed geometry of a charged state, D^{+}-A^{-}, does not involve significant geometrical changes as compared to the equilibrium geometry of the ground state.[79]

3 Results and Discussion

First, we discuss ground-state properties and compare main energetic, electronic, and structural parameters of the TPA-M@C_{80} structures. Then, a classification of excited states is provided. Finally, the driving force is examined to determine the most exergonic and endergonic processes.

3.1 Properties in the ground state

The ground-state geometries and electronic properties of the TPA-M@C_{80} structures are quite similar. For M = Sc_3N, Sc_3CH, Sc_3NC, Sc_4O_2, and Sc_4O_3, the charge on C_{80} ranges from -2.0 to -1.7 whereas the corresponding charge on the metallic cluster changes from +1.9 to +1.6, respectively. The charge on TPA is +0.1. The molecular dipole moment is found in the range from 5.0 to 6.6 D. The solvation energies, ΔG_{sol}, range from -0.74 to -0.71 eV. In Table S3, we separately compare the isolated structures of TPA and C_{80} with those in the complexes. The small values of RMSD suggest that both the TPA fragment and the fullerene cage do not show significant geometrical differences. Also, the shortest distance between the nitrogen atom in TPA and a carbon atom in C_{80} ranges from 7.6 to 7.9 Å. This difference is expected to have a negligible effect on the electronic properties of excited states (Table S4 summarizes the electronic and structural characteristics of the TPA-M@C_{80} structures in the ground state).

3.2 Characterization of excited states

The nature of excited states is studied within a two-fragment model. The fragments are TPA (electron donor) and M@C_{80} (electron acceptor). For any excited state, four parameters were calculated: X_{TPA} and $X_{M@C80}$ characterize exciton localization on the fragments; CT is the total amount of the electron density transferred from TPA to M@C_{80} and back by excitation, CT = q(D→A) + q(A→D); Δq is the charge separation from donor to acceptor sites, Δq = q(D→A) - q(A→D). In line with this scheme, several types of excited states can be distinguished in TPA-M@C_{80}. (i) Locally excited (**LE**) states TPA-[M@C_{80}]* where the electronic transition occurs on the acceptor, $X_{M@C80} > 0.9$; (ii) **LE** states TPA*-[M@C_{80}] where the electronic transition occurs on the donor, $X_{TPA} > 0.9$; (iii) delocalized excitonic states, where the $X_{M@C80}$ and X_{TPA} values are comparable; (iv) electronic transitions corresponding to **CS** states (D-A→D^+-A^-), $\Delta q > 0.9$ and $X_{M@C80}$ and X_{TPA} values are small; (v) Mixed excited (**ME**) states that have contributions of both **LE** and **CS** states.

Our calculations of TPA-Sc_3N@C_{80} suggest that 100 lowest singlet excited states in the complex lie in the energy region of 1.6-4.1 eV in the gas phase. Most of these excited states are **LE** states TPA-[Sc_3N@C_{80}]*. Three **CS** states [TPA]$^+$-[Sc_3N@C_{80}]$^-$ are found at 3.18, 3.71, and 4.06 eV. Five excited states are **ME** states that lie at nearly 3.8 eV. TPA*-[Sc_3N@C_{80}] states corresponding to excitation of the donor lie higher than 4.1 eV. The rest of the structures under study show a population of excited states similar to TPA-Sc_3N@C_{80}, and a detailed characterization of the lowest 100 singlet and 60 triplet excited states in every TPA-M@C_{80} complex is provided in Tables S5 and S6.

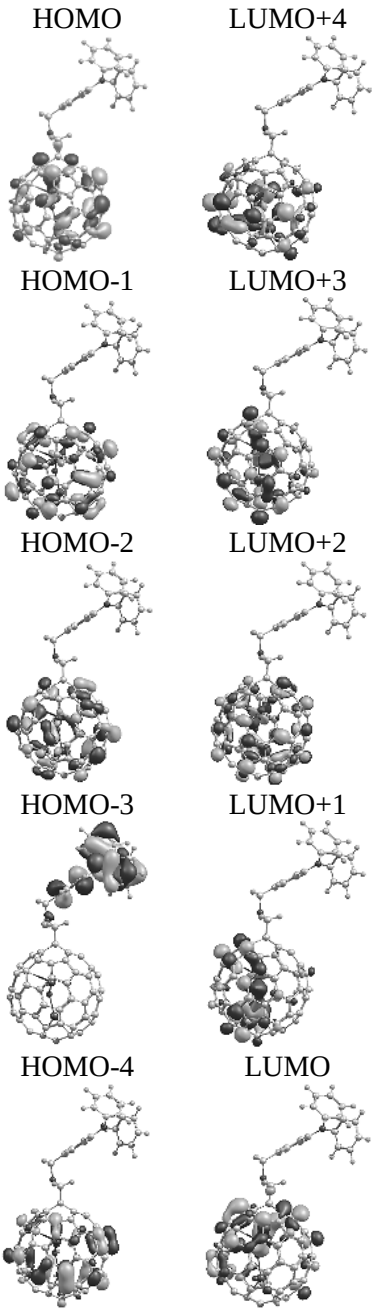

Figure 2 Frontier molecular orbitals in TPA-$Sc_3N@C_{80}$.

Most electronic transitions occur at the $M@C_{80}$ acceptor since many frontier molecular orbitals are mainly localized at this fragment (for instance, see Figure 2 for the case of TPA-$Sc_3N@C_{80}$). There are a few excited states with significant contribution of CS configurations; that is, excited states resulting from an electronic transition where the main orbital contribution is a HOMO-X (located at TPA) to LUMO+Y (situated at $M@C_{80}$). In Table 1, the HOMO-to-LUMO transitions in the gas phase are reported for the lowest locally excited ($\mathbf{LE}_1$) and charge-separated ($\mathbf{CS}_1$) states, as well as the excitation energy, oscillator strength, and dipole moment associated to such states.

In all cases, singlet **LE**$_1$ is formed from a HOMO→LUMO excitation with an energy cost ranging from 1.2 to 1.7 eV. Moreover, the dipole moment in **LE**$_1$ remains similar to the dipole moment in the ground state for every TPA-M@C_{80} structure, ~6.0 D, with the largest deviation for TPA-Sc_4O_3@C_{80}. On the other hand, an excited state generated from a HOMO-X→LUMO (X = 1, 2, or 3) transition corresponds to singlet **CS**$_1$. These states are characterized by a dipole moment larger than 50.0 D. However, TPA-Sc_4O_2@C_{80} does not show any pure **CS** state and for our purposes we use an **ME** state with the largest contribution of CS, Δq=0.8 (see Table S6 for complete details. Besides, this state shows a dipole moment below 50.0 D). Nonetheless, the electronic transitions leading to **LE**$_1$ and **CS**$_1$ are orbitally forbidden. We note that **CS** states, $[TPA]^-$-$[M@C_{80}]^+$,[35,80,81] where an electron is transferred from M@C_{80} to TPA are considerably higher in energy than $[TPA]^+$-$[M@C_{80}]^-$, and thus they are not considered here.

Table 1 Excitation energy *Ex* in eV, HOMO(H)-LUMO(L) orbital contribution, oscillator strength *f*, and dipole moment μ in Debye of **LE**$_1$ and **CS**$_1$ in TPA-M@C_{80} in the gas phase.

M	Parameter	**LE**$_1$		**CS**$_1$	
		singlet	*triplet*	*singlet*	*triplet*
Sc_3N	*Ex*	1.647	1.391	3.179	3.175
	Transit.	H→L	H→L	H-3→L	H-3→L
	f	0.02		0.01	
	μ	4.9	5.5	53.8	53.3
Sc_3CH	*Ex*	1.608	1.360	3.143	3.140
	Transit.	H→L	H→L	H-3→L	H-3→L
	f	0.02		0.00	
	μ	5.6	5.9	53.1	43.1[b]
Sc_3NC	*Ex*	1.617	1.291	3.292	3.290
	Transit.	H→L	H-6→L+1[a]	H-2→L	H-2→L
	f	0.00		0.00	
	μ	7.8	6.0	52.2	54.0
Sc_4O_2	*Ex*	1.165	0.403	3.324	3.322
	Transit.	H→L	H→L	H-2→L	H-2→L
	f	0.01		0.01	
	μ	8.2	7.8	44.2[b]	52.9
Sc_4O_3	*Ex*	1.531	1.411	3.263	3.261
	Transit.	H→L	H→L	H-1→L	H-1→L
	f	0.00		0.00	
	μ	11.6	11.1	59.9	58.9

[a] For this EMF, the H→L transition leads to the second lowest-in-energy **LE**.

[b] Only in these two cases, an **ME** state was used with the largest contribution of CS, Δq=0.8.

Triplet **LE**$_1$ and **CS**$_1$ keep almost the same characteristics as the respective singlet states. One exception is for TPA-Sc_3NC@C_{80}, where a HOMO→LUMO excitation leads to the second triplet **LE**. Another difference is the dipole moment lower than 50.0 D for the triplet **CS**$_1$ in TPA-Sc_3CH@C_{80} and singlet **CS**$_1$ in TPA-Sc_4O_2@C_{80}. As mentioned before, these triplet and singlet **CS** states are indeed **ME** states with a large contribution of CS, Δq = 0.8.

3.3 Photoinduced charge transfer in TPA-M@C_{80}

After light absorption (Eq. (4)) by the complex in the ground state, an **LE** state $X_{M@C80}$ is generated. Then, very fast internal conversion leads to **LE**$_1$. This state may be involved in the CS process (Eq. (5)) forming **CS**$_1$. In turn, this state decays to the ground state (Eq. (6)) leading to charge recombination:

$$TPA - M@C_{80} + h\nu \rightarrow TPA - [M@C_{80}]^* \quad (4)$$

$$TPA - [M@C_{80}]^* \rightarrow [TPA]^+ - [M@C_{80}]^- \quad (5)$$

$$[TPA]^+ - [M@C_{80}]^- \rightarrow TPA - M@C_{80} \quad (6)$$

Below we consider these processes in more detail.

The driving force of CS reactions is estimated as the energy difference between **LE**$_1$ and **CS**$_1$. The comparison between excitation energies computed in the gas phase and benzonitrile indicates that there are no significant changes in the position of **LE** states (the shifts are smaller than 0.1 eV. Complete details for all the transition energies for every TPA-M@C_{80} structure are provided in Table S7). In contrast, **CS** states are strongly stabilized due to the solvent (from 1.0 to 1.8 eV). In the case of TPA-Sc_3N@C_{80}, in benzonitrile the energy of **CS**$_1$ decreases by 1.64 eV. Then, **LE**$_1$ and **CS**$_1$ are found at 1.64 and 1.54 eV above the ground state. These estimates are in good agreement with the experimental energies of 1.50 and 1.45 eV, respectively.[36,79] **LE**$_1$ and **CS**$_1$ levels in the solvated complexes are depicted in Figure 3.

In the case of singlet excited states (Figure 3a), the CS driving forces are 0.10, 0.08, -0.25, -1.19, and -0.06 eV for TPA-M@C_{80} with M being Sc_3N, Sc_3CH, Sc_3NC, Sc_4O_2, and Sc_4O_3, respectively. CS reactions may occur effectively in the structures containing Sc_3N and Sc_3CH inside the C_{80} cage because these processes are exergonic; unlike the endergonic CS occurring in the systems involving Sc_3CN and Sc_4O_2. The CS process in TPA-Sc_4O_3@C_{80} is only slightly endergonic, ΔG = 0.06 eV, therefore it can also occur.

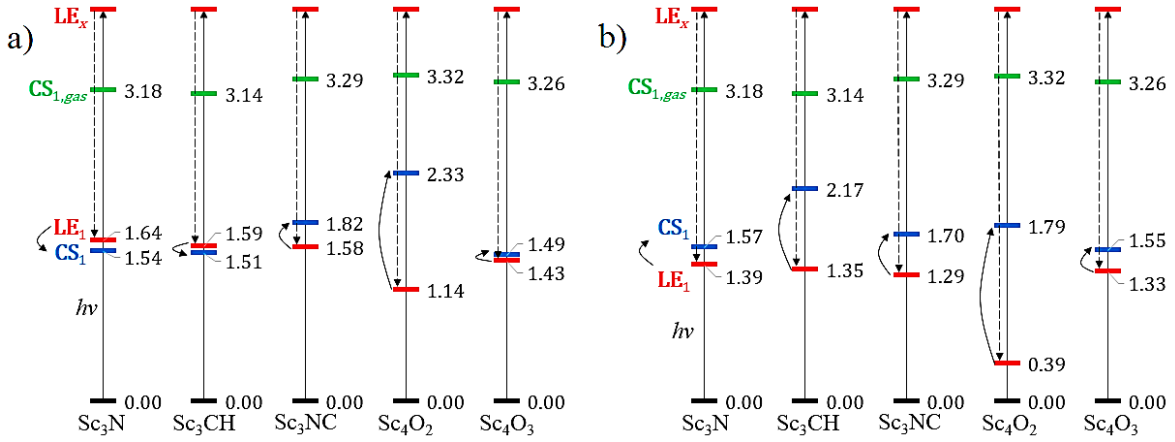

Figure 3 LE$_1$ and **CS$_1$** energies of TPA-M@C_{80} solvated in benzonitrile. The absorption of a photon leads to the formation of a high-energy excited state **LE**$_x$ (in red), which is immediately relaxed to the lowest **LE**$_1$ (in red). Then **LE**$_1$ may decay to the charge transfer character state **CS**$_1$ (in blue). The energy of **CS**$_1$ in the gas phase is also shown (in green). a) Singlet excited states; b) triplet excited states. Energies in eV.

In the case of triplet excited states (Figure 3b), we assume that the metal cluster generates the formation of triplet states by intersystem crossing from singlet **LE**$_1$ to triplet **LE**$_1$. Then, the CS driving forces forming triplet **CS**$_1$ are -0.18, -0.82, -0.42, -1.40, and -0.22 eV for TPA-M@C_{80} with M being Sc_3N, Sc_3CH, Sc_3NC, Sc_4O_2, and Sc_4O_3, respectively. Accordingly, CS reactions certainly does not occur following a triplet reaction pathway because they are endergonic processes. Furthermore, the CS reaction from singlet **LE**$_1$ to triplet **CS**$_1$ is an uphill process in every TPA-M@C_{80} structure excepting TPA-Sc_3N@C_{80}, in which such a process is slightly favored by 0.07 eV. Nevertheless, the singlet-to-triplet spin-crossing from a neutral to a charged state is expected to be not allowed due to the small spin-coupling.

Even though there are no experimental evidence for the CS reaction in TPA-M@C_{80} (except for M = Sc_3N), available electrochemical data can be used to approximate the value of **CS**$_1$ (see Eq. 6) in the following way:[82]

$$\boldsymbol{CS}_1 = E_{ox}^{TPA} + E_{red}^{M@C80} + C \qquad (7)$$

where $E_{ox/red}$ are the redox potentials of TPA and M@C_{80}, respectively, and the term C describes the solvent effects that are expected to be very similar in the considered TPA-M@C_{80} structures. Equation (7) suggests that the difference between **CS**$_1$ in TPA-M@C_{80} and **CS**$_1$ in TPA-Sc_3N@C_{80} is determined by the difference of the reduction potentials; $\boldsymbol{CS}_1^{TPA-M@C80} - \boldsymbol{CS}_1^{TPA-Sc3N@C80} = E_{red}^{M@C80} - E_{red}^{Sc3N@C80}$. The reduction potentials for M@C_{80} are experimentally known.[58,83–85] We noticed that the difference of the **CS**$_1$ values calculated in this report is concomitant with the experimental data (the largest deviation is found for TPA-Sc_4O_2@C_{80}) and thus supports our predictions (see Table S8 for details).

4 Conclusions

In our study, we examined the driving force of charge separation (CS) in TPA-M@C_{80} species with M = Sc_3N, Sc_3CH, Sc_3NC, Sc_4O_2, and Sc_4O_3. Since CS is one of the most important processes occurring in dye-sensitized solar cells, we expect that our study can provide valuable information for the development of more efficient dye-sensitized solar cells containing endohedral metallofullerenes. On the basis of TD CAM-B3LYP calculations we have found that:

(i) Three types of excited states are mainly generated in TPA-M@C_{80} after light absorption: excitons localized at the acceptor, states with strong charge transfer (CT) character (large separation of charge between the donor and acceptor sites) $[TPA]^+$-$[M@C_{80}]^-$, and, finally, mixed states including both local and CT excitations.

(ii) Solvent effects are found to be crucial for an efficient population of singlet and triplet **CS** states. Indeed, charge separation does not take place in the gas phase or in solvents of low polarity.

(iii) In benzonitrile, the systems containing Sc_3N, Sc_3CH, and Sc_4O_3 have been found to facilitate the formation of **CS** states. In contrast, no efficient electron transfer is expected for structures containing Sc_3NC and Sc_4O_2.

(iv) Even though the formation of triplet states is promoted by the metal cluster through intersystem crossing, the decay of these states through electron transfer does not efficiently occur. Triplet **CS** states are more likely generated in the species containing Sc_3N and Sc_4O_3 inside C_{80}.

Acknowledgements

We are grateful for financial support from the Spanish Ministerio de Economía y Competitividad (MINECO) (Projects CTQ2014-54306-P and CTQ2015-69363-P), the Catalan DIUE (Project 2014SGR931, ICREA Academia 2014 Award to MS, and Xarxa de Referència en Química Teòrica i Computacional), and the FEDER fund (UNGI10-4E-801). JPM acknowledges the Mexican National Council of Science and Technology (CONACYT) for his PhD fellowship (register/application number 217067/312543).

Supporting Information

Detailed information of the structure, energetics, electronic properties, and electron transfer parameters for the systems under consideration.

References

[1] B. O'Regan, M. Grätzel, *Nature* **1991**, *353*, 737–740.
[2] D. Jariwala, V. K. Sangwan, L. J. Lauhon, T. J. Marks, M. C. Hersam, *Chem. Soc. Rev.* **2013**, *42*, 2824–2860.
[3] S. Günes, H. Neugebauer, N. S. Sariciftci, *Chem. Rev.* **2007**, *107*, 1324–1338.
[4] J. Yan, B. R. Saunders, *RSC Adv.* **2014**, *4*, 43286–43314.
[5] B. R. Saunders, M. L. Turner, *Adv. Colloid Interface Sci.* **2008**, *138*, 1–23.
[6] S. A. Berhe, H. B. Gobeze, S. D. Pokharel, E. Park, W. J. Youngblood, *ACS Appl. Mater. Interfaces* **2014**, *6*, 10696–10705.
[7] G. Chen, J. Seo, C. Yang, P. N. Prasad, *Chem. Soc. Rev.* **2013**, *42*, 8304–8338.
[8] J. L. Delgado, P.-A. Bouit, S. Filippone, M. A. Herranz, N. Martín, *Chem. Commun.* **2010**, *46*, 4853–4865.
[9] C. A. Echeverry, R. Cotta, E. Castro, A. Ortiz, L. Echegoyen, B. Insuasty, *RSC Adv.* **2015**, *5*, 60823–60830.
[10] G. V. Dubacheva, C.-K. Liang, D. M. Bassani, *Coord. Chem. Rev.* **2012**, *256*, 2628–2639.
[11] Y. He, Y. Li, *Phys. Chem. Chem. Phys.* **2011**, *13*, 1970–1983.
[12] X. Lu, L. Feng, T. Akasaka, S. Nagase, *Chem. Soc. Rev.* **2012**, *41*, 7723–7760.
[13] M. Rudolf, S. V Kirner, D. M. Guldi, *Chem. Soc. Rev.* **2016**, *45*, 612–630.
[14] M. S. Mauter, M. Elimelech, *Environ. Sci. Technol.* **2008**, *42*, 5843–5859.
[15] P. Kumar, S. Chand, *Prog. Photovoltaics Res. Appl.* **2012**, *20*, 377–415.
[16] G. Yu, J. Gao, J. C. Hummelen, F. Wudl, A. J. Heeger, *Science* **1995**, *270*, 1789–1791.
[17] B. C. Thompson, J. M. J. Fréchet, *Angew. Chem. Int. Ed.* **2008**, *47*, 58–77.
[18] P. W. M. Blom, V. D. Mihailetchi, L. J. A. Koster, D. E. Markov, *Adv. Mater.* **2007**, *19*, 1551–1566.
[19] J. Peet, J. Y. Kim, N. E. Coates, W. L. Ma, D. Moses, A. J. Heeger, G. C. Bazan, *Nat. Mater.* **2007**, *6*, 497–500.

[20] Y. Huang, E. J. Kramer, A. J. Heeger, G. C. Bazan, *Chem. Rev.* **2014**, *114*, 7006–7043.
[21] J. L. Segura, N. Martin, D. M. Guldi, *Chem. Soc. Rev.* **2005**, *34*, 31–47.
[22] J. Guo, H. Ohkita, H. Benten, S. Ito, *J. Am. Chem. Soc.* **2010**, *132*, 6154–6164.
[23] C. Groves, O. G. Reid, D. S. Ginger, *Acc. Chem. Res.* **2010**, *43*, 612–620.
[24] G. Li, V. Shrotriya, J. Huang, Y. Yao, T. Moriarty, K. Emery, Y. Yang, *Nat. Mater.* **2005**, *4*, 864–868.
[25] H. Ohkita, S. Cook, Y. Astuti, W. Duffy, S. Tierney, W. Zhang, M. Heeney, I. McCulloch, J. Nelson, D. D. C. Bradley, et al., *J. Am. Chem. Soc.* **2008**, *130*, 3030–3042.
[26] I.-W. Hwang, D. Moses, A. J. Heeger, *J. Phys. Chem. C* **2008**, *112*, 4350–4354.
[27] X. Ai, M. C. Beard, K. P. Knutsen, S. E. Shaheen, G. Rumbles, R. J. Ellingson, *J. Phys. Chem. B* **2006**, *110*, 25462–25471.
[28] G. Sauvé, R. Fernando, *J. Phys. Chem. Lett.* **2015**, *6*, 3770–3780.
[29] I. Gutiérrez-González, B. Molina-Brito, A. W. Götz, F. L. Castillo-Alvarado, J. I. Rodríguez, *Chem. Phys. Lett.* **2014**, *612*, 234–239.
[30] J. I. Rodríguez, C. F. Matta, E. A. Uribe, A. W. Götz, F. L. Castillo-Alvarado, B. Molina-Brito, *Chem. Phys. Lett.* **2016**, *644*, 157–162.
[31] Y. Kawashima, K. Ohkubo, S. Fukuzumi, *J. Phys. Chem. A* **2013**, *117*, 6737–6743.
[32] S. Stevenson, G. Rice, T. Glass, K. Harich, F. Cromer, M. R. Jordan, J. Craft, E. Hadju, R. Bible, M. M. Olmstead, et al., *Nature* **1999**, *401*, 55–57.
[33] J. R. Pinzón, M. E. Plonska-Brzezinska, C. M. Cardona, A. J. Athans, S. S. Gayathri, D. M. Guldi, M. A. Herranz, N. Martín, T. Torres, L. Echegoyen, *Angew. Chem. Int. Ed.* **2008**, *47*, 4173–4176.
[34] J. R. Pinzón, C. M. Cardona, M. A. Herranz, M. E. Plonska-Brzezinska, A. Palkar, A. J. Athans, N. Martín, A. Rodríguez-Fortea, J. M. Poblet, G. Bottari, et al., *Chem. Eur. J.* **2009**, *15*, 864–877.
[35] O. Trukhina, M. Rudolf, G. Bottari, T. Akasaka, L. Echegoyen, T. Torres, D. M. Guldi, *J. Am. Chem. Soc.* **2015**, *137*, 12914–12922.
[36] J. R. Pinzón, D. C. Gasca, S. G. Sankaranarayanan, G. Bottari, T. Torres, D. M. Guldi, L. Echegoyen, *J. Am. Chem. Soc.* **2009**, *131*, 7727–7734.
[37] A. S. D. Sandanayaka, H. Sasabe, Y. Araki, Y. Furusho, O. Ito, T. Takata, *J. Phys. Chem. A* **2004**, *108*, 5145–5155.
[38] V. Coropceanu, J. Cornil, D. A. da Silva Filho, Y. Olivier, R. Silbey, J.-L. Brédas, *Chem. Rev.* **2007**, *107*, 926–952.
[39] J. Preat, *J. Phys. Chem. C* **2010**, *114*, 16716–16725.
[40] G. Wu, F. Kong, Y. Zhang, X. Zhang, J. Li, W. Chen, W. Liu, Y. Ding, C. Zhang, B. Zhang, et al., *J. Phys. Chem. C* **2014**, *118*, 8756–8765.
[41] J. Xu, L. Wang, G. Liang, Z. Bai, L. Wang, W. Xu, X. Shen, *Bull. Korean Chem. Soc.* **2010**, *31*, 2531–2536.
[42] Z. Ning, Q. Zhang, W. Wu, H. Pei, B. Liu, H. Tian, *J. Org. Chem.* **2008**, *73*, 3791–3797.
[43] N. Martín, L. Sánchez, B. Illescas, I. Pérez, *Chem. Rev.* **1998**, *98*, 2527–2548.
[44] F. D'Souza, R. Chitta, A. S. D. Sandanayaka, N. K. Subbaiyan, L. D'Souza, Y. Araki, O. Ito, *J. Am. Chem. Soc.* **2007**, *129*, 15865–15871.
[45] K. Stranius, V. Iashin, T. Nikkonen, M. Muuronen, J. Helaja, N. Tkachenko, *J. Phys. Chem. A* **2014**, *118*, 1420–1429.
[46] B. M. Illescas, N. Martín, *J. Org. Chem.* **2000**, *65*, 5986–5995.
[47] N. Martín, *Chem. Commun.* **2006**, 2093–2104.
[48] C. Thilgen, F. Diederich, *Chem. Rev.* **2006**, *106*, 5049–5135.
[49] N. Martín, I. Pérez, L. Sánchez, C. Seoane, *J. Org. Chem.* **1997**, *62*, 5690–5695.
[50] Z. Zhou, P. A. Magriotis, *Org. Lett.* **2005**, *7*, 5849–5851.
[51] S. H. Hoke, J. Molstad, D. Dilettato, M. J. Jay, D. Carlson, B. Kahr, R. G. Cooks, *J. Org. Chem.* **1992**, *57*, 5069–5071.

[52] C. Bingel, *Chem. Ber.* **1993**, *126*, 1957–1959.
[53] M. N. Chaur, F. Melin, A. L. Ortiz, L. Echegoyen, *Angew. Chem. Int. Ed.* **2009**, *48*, 7514–7538.
[54] S. Osuna, M. Swart, M. Solà, *Phys. Chem. Chem. Phys.* **2011**, *13*, 3585–3603.
[55] M. Chergui, *Dalton Trans.* **2012**, *41*, 13022–13029.
[56] M. Liedtke, A. Sperlich, H. Kraus, A. Baumann, C. Deibel, M. J. M. Wirix, J. Loos, C. M. Cardona, V. Dyakonov, *J. Am. Chem. Soc.* **2011**, *133*, 9088–9094.
[57] M. Krause, F. Ziegs, A. A. Popov, L. Dunsch, *ChemPhysChem* **2007**, *8*, 537–540.
[58] T.-S. Wang, L. Feng, J.-Y. Wu, W. Xu, J.-F. Xiang, K. Tan, Y.-H. Ma, J.-P. Zheng, L. Jiang, X. Lu, et al., *J. Am. Chem. Soc.* **2010**, *132*, 16362–16364.
[59] S. Stevenson, M. A. Mackey, M. A. Stuart, J. P. Phillips, M. L. Easterling, C. J. Chancellor, M. M. Olmstead, A. L. Balch, *J. Am. Chem. Soc.* **2008**, *130*, 11844–11845.
[60] B. Q. Mercado, M. M. Olmstead, C. M. Beavers, M. L. Easterling, S. Stevenson, M. A. Mackey, C. E. Coumbe, J. D. Phillips, J. P. Phillips, J. M. Poblet, et al., *Chem. Commun.* **2010**, *46*, 279–281.
[61] A. A. Popov, S. Yang, L. Dunsch, *Chem. Rev.* **2013**, *113*, 5989–6113.
[62] M. J. Frisch, G. W. Trucks, H. B. Schlegel, G. E. Scuseria, M. A. Robb, J. R. Cheeseman, G. Scalmani, V. Barone, B. Mennucci, G. A. Petersson, et al., **2009**.
[63] T. Yanai, D. P. Tew, N. C. Handy, *Chem. Phys. Lett.* **2004**, *393*, 51–57.
[64] D. Andrae, U. Häußermann, M. Dolg, H. Stoll, H. Preuß, *Theor. Chim. Acta* **1990**, *77*, 123–141.
[65] M. Dolg, U. Wedig, H. Stoll, H. Preuss, *J. Chem. Phys.* **1987**, *86*, 866.
[66] A. Klamt, *J. Phys. Chem.* **1995**, *99*, 2224–2235.
[67] M. Garcia-Borràs, S. Osuna, J. M. Luis, M. Swart, M. Solà, *Chem. Eur. J.* **2013**, *19*, 14931–14940.
[68] L. Basurto, F. Amerikheirabadi, R. Zope, T. Baruah, *Phys. Chem. Chem. Phys.* **2015**, *17*, 5832–5839.
[69] A. D. Becke, *J. Chem. Phys.* **1993**, *98*, 5648.
[70] C. Lee, W. Yang, R. G. Parr, *Phys. Rev. B* **1988**, *37*, 785–789.
[71] J. P. Martínez, S. Osuna, M. Solà, A. Voityuk, *Theor. Chem. Acc.* **2015**, *134*, 12.
[72] A. Troisi, *Faraday Discuss.* **2013**, *163*, 377–392.
[73] S. Few, J. M. Frost, J. Kirkpatrick, J. Nelson, *J. Phys. Chem. C* **2014**, *118*, 8253–8261.
[74] T. Liu, D. L. Cheung, A. Troisi, *Phys. Chem. Chem. Phys.* **2011**, *13*, 21461.
[75] F. Plasser, M. Wormit, A. Dreuw, *J. Chem. Phys.* **2014**, *141*, 024106.
[76] J. Tomasi, B. Mennucci, R. Cammi, *Chem. Rev.* **2005**, *105*, 2999–3093.
[77] J. L. Pascual-ahuir, E. Silla, I. Tuñon, *J. Comput. Chem.* **1994**, *15*, 1127–1138.
[78] A. Klamt, *J. Phys. Chem.* **1996**, *100*, 3349–3353.
[79] J. P. Martínez, M. Solà, A. A. Voityuk, *J. Comput. Chem.* **2016**, *37*, 1396–1405.
[80] D. M. Guldi, L. Feng, S. G. Radhakrishnan, H. Nikawa, M. Yamada, N. Mizorogi, T. Tsuchiya, T. Akasaka, S. Nagase, M. Ángeles Herranz, et al., *J. Am. Chem. Soc.* **2010**, *132*, 9078–9086.

[81] L. Feng, S. G. Radhakrishnan, N. Mizorogi, Z. Slanina, H. Nikawa, T. Tsuchiya, T. Akasaka, S. Nagase, N. Martín, D. M. Guldi, *J. Am. Chem. Soc.* **2011**, *133*, 7608–7618.
[82] A. Amini, A. Harriman, *J. Photochem. Photobiol. C* **2003**, *4*, 155–177.
[83] B. Elliott, L. Yu, L. Echegoyen, *J. Am. Chem. Soc.* **2005**, *127*, 10885–10888.
[84] K. Junghans, M. Rosenkranz, A. A. Popov, *Chem. Commun.* **2016**, *52*, 6561–6564.
[85] A. A. Popov, N. Chen, J. R. Pinzón, S. Stevenson, L. A. Echegoyen, L. Dunsch, *J. Am. Chem. Soc.* **2012**, *134*, 19607–19618.

GRAPHIC FOR TABLE OF CONTENTS